



# A Direct Borohydride/Hydrogen Peroxide Fuel Cell with Reduced Alkali Crossover

R. K. Raman<sup>1</sup>, and A. K. Shukla<sup>1,2\*</sup>

<sup>1</sup> Solid State and Structural Chemistry Unit, Indian Institute of Science, Bangalore-560 012, India

<sup>2</sup> Central Electrochemical Research Institute, Karaikudi-630003, India

Received May 25, 2006; accepted November 30, 2006

## Abstract

A direct borohydride/hydrogen peroxide fuel cell, employing a misch-metal alloy anode and carbon-supported lead sulfate (PbSO<sub>4</sub>/C) cathode with a Nafion<sup>®</sup>-961 membrane electrolyte, is reported. The use of a Nafion<sup>®</sup>-961 membrane electrolyte in the fuel cell lessens the crossover of aqueous sodium hydroxide from the anode to cathode. Initial results indicate that the fuel cell exhibits a maximum power density of 10 mW cm<sup>-2</sup> at an operating voltage of 0.77 V with an oxidant utilization of about 80% at 25 °C. The fuel cell also avoids the use of noble-metal catalysts. The unique combina-

tion of sodium borohydride and hydrogen peroxide, both of which are in aqueous form, paves the way for a convenient unitized refueling design that is inherently compact compared to fuel cells that use gaseous reactants. Such a fuel cell is expected to find application in situations where anaerobic conditions prevail, e.g., in submersible and space applications.

**Keywords:** Direct Borohydride/Hydrogen Peroxide Fuel Cell, Hydrogen Peroxide, Lead Sulfate, Nafion<sup>®</sup>-117, Nafion<sup>®</sup>-961

## 1 Introduction

Hydrogen is not available freely in nature. Accordingly, it has to be generated from a readily available hydrogen-carrying fuel, such as natural gas, which requires reforming [1]. However, such a process leads to the generation of hydrogen contaminated with carbon monoxide, which even at minute levels is detrimental to the performance of fuel cells [2]. Pure hydrogen can be generated through the electrolysis of water but hydrogen thus generated needs to be stored as compressed/liquefied gas, which is expensive [3]. Therefore, certain hydrogen carrying organic fuels, such as methanol, ethanol, propanol, ethylene glycol, and diethyl ether, have been considered for fuelling PEFCs directly [4–7]. Amongst these, methanol (*specific energy* = 6.1 kWh kg<sup>-1</sup>) is the most attractive organic liquid. PEFCs directly fuelled with methanol are called solid-polymer-electrolyte direct methanol fuel cells (SPE-DMFCs) [5–7]. However, SPE-DMFCs suffer from methanol crossover across the polymer electrolyte membrane, affecting cathode performance [8]. Furthermore, SPE-DMFCs have inherent limitations, their low open-circuit potential and low electrochemical activity [8]. An obvious solution to these

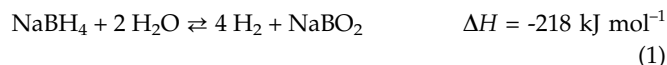
problems is to explore other promising hydrogen-carrying chemicals to directly fuel PEFCs.

Reversible metal hydrides, obtained by directly reacting hydrogen with certain metals, e.g., titanium, iron, manganese, nickel, and chromium, or their alloys, have been reported as hydrogen storage materials [9]. However, these materials are not potentially attractive apart from their high volumetric energy density. Alternatives to reversible metal hydrides are alkali metal hydrides, which react with water to release hydrogen and produce metal hydroxides. However, alkali metal hydrides are both corrosive and toxic, and need to be disposed of safely. Besides, the energy required to manufacture and transport alkali metal hydrides is greater than that realized by the fuel cell [9]. Another promising material, with a hydrogen content as high as 20 wt.%, is ammonia borane (NH<sub>3</sub>BH<sub>3</sub>), which is stable at ambient temperatures and releases hydrogen only when heated beyond 150 °C [10]. Recent research suggests that the hydriding / dehydriding

[\*] Corresponding author, shukla@sscu.iisc.ernet.in

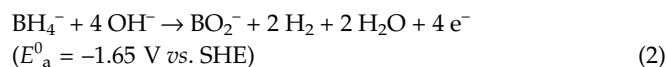
activity of TiF<sub>3</sub> doped NaAlH<sub>4</sub>, LiNH<sub>2</sub>, and LiBH<sub>4</sub> to be about 5 wt.-% [11, 12].

In recent years, there has been clear interest in the use of sodium tetrahydridoborate or sodium borohydride (NaBH<sub>4</sub>) with a hydrogen content of approximately 11 wt.-% for fueling PEFCs, both directly [13–27] and indirectly [28–29]. Such PEFCs are referred to as direct and indirect borohydride fuel cells. In an indirect borohydride fuel cell, reacting NaBH<sub>4</sub> with water in the presence of a catalyst produces hydrogen in accordance with the following reaction.

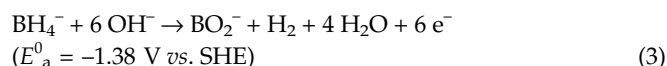


The hydrogen produced is fed to the anode of the indirect borohydride fuel cell. In contrast, in the direct borohydride fuel cell (DBFC), an alkaline aqueous solution of sodium borohydride is directly fed to its anode, which is oxidized to NaBO<sub>2</sub>, delivering electrical energy.

The anodic oxidation of borohydride has been studied on Ni, Pt, Pd, Ni<sub>2</sub>B, Au, and on noble metal alloys by various groups [13, 17–27, 30–32]. Indig and Snyder were the first to identify sodium borohydride as a fuel [13]. These authors used a Ni anode with 80% porosity and reported a polarization voltage of –1.125 V vs. Hg/HgO at a load current density of 200 mA cm<sup>-2</sup> [13]. A coulombic efficiency of 49% was obtained at load current densities below 100 mA cm<sup>-2</sup>, where a 4-electron reaction takes place,



Kubokawa et al. studied the oxidation of borohydride over Pd and observed a 6-electron reaction per borohydride ion, as shown below [31].

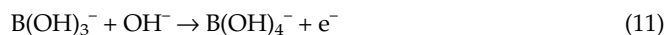
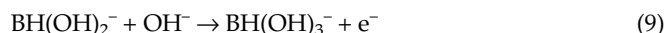
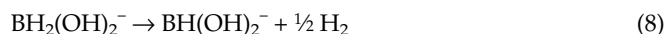
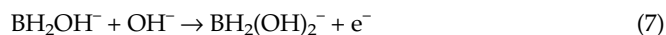


It should be noted that the electromotive force of DBFC increases as the number of electrons utilized per BH<sub>4</sub><sup>-</sup> ion decreases from 8. Elder and Hickling [32] have proposed a reaction path for the oxidation of BH<sub>4</sub><sup>-</sup> on Pt. According to them, the BH<sub>4</sub><sup>-</sup> ion hydrolyses to a stable BH<sub>3</sub>OH<sup>-</sup> intermediate that undergoes partial oxidation, which, on subsequent hydrolysis, yields 2–4 electrons per BH<sub>4</sub><sup>-</sup> ion. Amendola et al. [17] were the first to report a OH<sup>-</sup>-ion conducting anion exchange membrane-based borohydride-air fuel cell. Their fuel cell used a Au (97)-Pt (3) alloy for the oxidation of borohydride, with a power density close to 60 mW cm<sup>-2</sup> at 70 °C. They reported a utilization of about 7.5-electrons per borohydride ion, during the borohydride oxidation on the Au-Pt alloy. However, this borohydride-air fuel cell suffers from borohydride crossover across the anion exchange membrane. It should be mentioned that Au belongs to a group of metals with a high hydrogen overpotential on which the formation

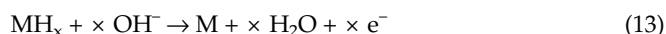
of surface hydrides or hydrogen adsorption occur readily. Thus, the use of Au as an electrocatalyst for BH<sub>4</sub><sup>-</sup> oxidation could avoid the hydrolysis of BH<sub>4</sub><sup>-</sup> but the operating cell voltage and power output would be low.

The use of hydrogen storage alloys as anodes in borohydride fuel cells has also been explored in the literature [18–24]. The role of the borohydride ion was to replenish the hydrogen within the lattice of the alloys, which then acts as the anode in the fuel cell. Li et al. [19] reported the use of a Zr-Ni hydrogen storage alloy as an anode material akin to those used in nickel-metal hydride batteries. The BH<sub>4</sub><sup>-</sup> crossover problem was reduced by adopting a divided cell configuration, using a Nafion<sup>®</sup> membrane as the electrolyte to separate the fuel from the cathode. A power density value as high as 160 mW cm<sup>-2</sup> was achieved at 70 °C.

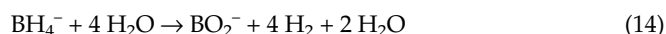
Borohydride oxidation takes place on the metal hydride surface, with associated hydrogen evolution, through the sequence of steps described below [15].



The hydrogen generated is stored in a hydrogen storage alloy anode, as MH<sub>x</sub>, which is involved in the discharge reaction as follows.



The following side-reaction (14), which occurs both at open-circuit and during cell operation, also reduces fuel utilization.



It is noteworthy that the DBFC operates at a potential cathodic to the standard potential for the hydrogen evolution reaction in a basic medium. This leads to the evolution of hydrogen at the anode during borohydride oxidation [33]. The relative rates of these reactions depend on the anodic materials, applied potentials, and chemical states of the anodic surfaces. Hydrogen evolution limits the efficiency of the

DBFC, but this effect can be lessened by the use of materials with high hydrogen overpotentials, inhibitors/additives [34], and by the surface treatment of the metal hydrides [35].

In recent years, there has been rapid progress in the development of direct borohydride fuel cells [17, 21–24, 26, 35–37]. Two types of direct borohydride fuel cell have been reported in the literature, namely, direct borohydride/air fuel cells [17, 21, 38] and direct borohydride/hydrogen peroxide fuel cells [24, 39, 40].

In an acidic medium, hydrogen peroxide can be reduced by either of the following routes [41].

(i) Direct reduction of  $\text{H}_2\text{O}_2$  to  $\text{H}_2\text{O}$ :



(ii) Chemical decomposition of  $\text{H}_2\text{O}_2$ , followed by reduction to  $\text{H}_2\text{O}$ :



However, the reversible potential for  $\text{H}_2\text{O}_2$  reduction is difficult to measure, as the reactions involved are dependent on several factors, such as the electrolyte and the surface chemistry of the catalyst used. Besides, there is always some associated oxygen evolution when employing  $\text{H}_2\text{O}_2$  on various catalyst surfaces.

A direct borohydride/hydrogen peroxide fuel cell employs a misch-metal alloy as the anode and carbon-supported platinum (Pt/C) as the cathode, with a Nafion<sup>®</sup>-117 membrane as a separator-cum-electrolyte. However, hydrogen peroxide has been found to decompose on a Pt/C cathode [40]. Accordingly, attempts have been made to substitute for the Pt/C catalyst in direct borohydride/hydrogen peroxide fuel cells [39].

In a recent publication [39], carbon-supported lead sulfate ( $\text{PbSO}_4/\text{C}$ ) was demonstrated to be an effective cathode material for reducing hydrogen peroxide to water in an acidic medium in a direct borohydride fuel cell, where hydrogen peroxide reduction, mediated by  $\text{Pb(II)}/\text{Pb(II+x)}$  (where  $2 < x < 0$ ), commences around 0.75 V vs. SHE. However, in such a fuel cell,  $\text{PbSO}_4/\text{C}$  is susceptible to aqueous sodium hydroxide crossover from the anode to cathode across the Nafion<sup>®</sup>-117 membrane [42].

To prevent the aforementioned problem, as part of an on-going R&D program on direct borohydride fuel cells [24, 39, 40], this communication reports a direct borohydride fuel cell with a Nafion<sup>®</sup>-961 membrane electrolyte that reduces the crossover of sodium hydroxide from the anode to the cathode. Such a direct borohydride fuel cell can deliver a peak power density of 10 mW cm<sup>-2</sup> at 0.77 V while operating at 25 °C. This is comparable to the anticipated power density of about 9 mW cm<sup>-2</sup> for the direct methanol/hydrogen perox-

ide fuel cell [43]. Commercially, sodium borohydride is produced by the Brown-Schlesinger [44, 45] and Bayer [46, 47] processes. In the latter, sodium borohydride is synthesized batch-wise, combining borax, metallic sodium, and hydrogen in the presence of silica at 700 °C, yielding sodium silicate as the by-product. The synthesis temperature is an explosion hazard due to the rapid decomposition of borohydride. Recently, a modification to the Bayer process has been used, where sodium borohydride can be produced from a mixture of sodium borate and sodium hydroxide in the presence of magnesium hydride ( $\text{MgH}_2$ ), which exhibits a significantly higher conversion efficiency [48–54]. The estimated cost of sodium borohydride, thus produced, is estimated to be one tenth of its current price of \$ 50 per kg [48]. In the borohydride/hydrogen peroxide fuel cell reported here, it is possible to achieve a hydrogen peroxide utilization of about 80%. Although  $\text{PbSO}_4$  is not an environmentally friendly chemical [55], enough is known from the lead-acid battery industry to handle it safely.

## 2 Experimental

### 2.1 Preparation of the $\text{AB}_5$ Alloy and Carbon-Supported $\text{PbSO}_4$ Catalyst

In the direct borohydride fuel cell reported here,  $M_m$  (misch metal)  $\text{Ni}_{3.6}\text{Al}_{0.4}\text{Mn}_{0.3}\text{Co}_{0.7}$  alloy ( $M_m = \text{La-30 wt.-%, Ce-50 wt.-%, Nd-15 wt.-%, Pr-5 wt.-%}$ ) was used as the anode. The  $M_m \text{Ni}_{3.6}\text{Al}_{0.4}\text{Mn}_{0.3}\text{Co}_{0.7}$  alloy was prepared by arc-melting stoichiometric amounts of the constituent metals in a water-cooled copper crucible under an argon atmosphere. The alloy ingot obtained was mechanically pulverized to a fine powder, with a particle size of about 60  $\mu\text{m}$ .

To obtain  $\text{PbSO}_4/\text{C}$ , equimolar solutions of lead acetate and sulfuric acid were mixed in a beaker containing 4 wt.-% Vulcan XC-72R carbon. The carbon-supported lead sulfate formed was filtered, washed with a large volume of hot distilled-water, and dried in an air oven at 80 °C for 12 h.

### 2.2 Fabrication of Membrane Electrode Assemblies (MEAs)

MEAs were obtained by sandwiching a Nafion<sup>®</sup>-961 polymer electrolyte membrane between the anode and cathode, which allowed for the electrochemical characterization of the direct borohydride fuel cell (DBFC). Nafion<sup>®</sup>-961 membrane is a Teflon-fiber reinforced composite membrane with sulfonate (100  $\mu\text{m}$ ) and carboxylate (10  $\mu\text{m}$ ) polymer layers. Unlike Nafion<sup>®</sup>-117, the Nafion<sup>®</sup>-961 membrane reduces alkali crossover from the anode to cathode in the cell. The presence of the carboxylate layer in the Nafion<sup>®</sup>-961 membrane offers resistance to NaOH flow. If the flow of NaOH were not prevented, the cell would suffer from anode polarization due to NaOH loss and cathode polarization due to the neutralization of the acid present in the catholyte and the consequent increase in pH, which is not conducive to the operation of the cell reported in this study. Accordingly, Nafion<sup>®</sup>-961 facilitates

higher oxidant utilization at the cathode of the DBFC. Other commercially available membranes of this class belong to the Nafion<sup>®</sup>-900 and Nafion<sup>®</sup>-2000 series. Note that a slurry of the alloy, obtained by ultra-sonicating the required amount of alloy with 5 wt.-% Vulcan XC-72R carbon and 5 wt.-% of Nafion<sup>®</sup> solution in isopropyl alcohol, was pasted onto the carboxylate side of the membrane. Exposing the carboxylate side to the acid present in the catholyte produces carboxylic acid (weak acid); whose dissociation constant reduces due to the common ion effect of H<sup>+</sup>. Hence, the ionic conductivity of the carboxylate side of the membrane is reduced. The alloy catalyst loading was kept at 39 mg cm<sup>-2</sup>. The use of alloy particles of ca. 60 μm in size for the electrodes provides sufficient inter particle porosity for the necessary flux across the electrode. The cathode is comprised of PbSO<sub>4</sub>/C mixed with 10 wt.-% of Nafion<sup>®</sup> solution in isopropyl alcohol pasted onto the sulfonate layer of the membrane. The PbSO<sub>4</sub>/C loading at the cathode was kept at 8 mg cm<sup>-2</sup>. The membrane electrode assembly was obtained by hot-pressing the cathode and anode placed on either side of the Nafion<sup>®</sup>-961 membrane at 60 kg cm<sup>-2</sup> for 3 min at 125 °C.

The anode catalyst layer in the MEA was supported by a stainless steel mesh while the cathode of the MEA was supported by Toray carbon paper. Both the anode and cathode were contacted on their rear with fluid flow field plates machined from high-density graphite blocks in which holes connecting the main tank were machined to achieve the minimum mass-polarization in the DBFC, as shown in Figure 1. The free-space between the holes makes electrical contact with the rear of the electrode and helps conduct the current to the external circuit. The tanks supply alkaline sodium borohydride solution to the anode and acidified hydrogen peroxide to the cathode, through the holes. An aqueous sodium borohydride solution, 4 wt.-% NaBH<sub>4</sub> in 20 wt.-% aqueous NaOH (anolyte), was injected into the fuel tank, and a 2 M hydrogen peroxide solution in 1.5 M sulfuric acid and a

0.1 M orthophosphoric acid mixture (catholyte) were injected into the oxidant tank. Graphite blocks were also provided with electrical contacts. The active area of the DBFC was 9 cm<sup>2</sup>. A schematic of the DBFC is shown in Figure 1.

### 2.3 Electrochemical Characterization of the DBFC

Galvanostatic polarization data for the DBFC at 25 °C were recorded by injecting 7 ml of aq. alkaline NaBH<sub>4</sub> into the fuel tank and a similar amount of acidic hydrogen peroxide into the oxidant tank. The anode and cathode polarization data for the DBFC were obtained against a Hg/HgO, OH<sup>-</sup> (MMO) reference electrode placed in the fuel tank and a Hg/Hg<sub>2</sub>SO<sub>4</sub>/SO<sub>4</sub><sup>2-</sup> (MMS) reference electrode placed in the oxidant tank. The data are reported against SHE in an acidic medium.

To examine the effect of NaOH crossover on cathode polarization, while employing Nafion<sup>®</sup>-117 and Nafion<sup>®</sup>-961 membranes as the electrolyte, 4.5 ml of catholyte and 7 ml of anolyte were added to the respective chambers. Then, the DBFC was operated at a load current density of 10 mA cm<sup>-2</sup> and the change in the cathode potential was followed continuously until the end of the experiment, i.e., up to the inflection point. As PbSO<sub>4</sub> is not quite stable in alkali [42], gold electrodes were employed for the previously mentioned comparative study between the Nafion<sup>®</sup>-117 and Nafion<sup>®</sup>-961 membranes.

To determine the fuel efficiency for borohydride oxidation, 7 ml of alkaline NaBH<sub>4</sub> were injected into the fuel tank and 7 ml of acidic hydrogen peroxide were injected into the oxidant tank. Subsequently, the cell was operated at load current density values of 11 and 23 mA cm<sup>-2</sup>. The fuel efficiency of the DBFC was calculated from the data collected in monitoring the anode potential until an abrupt change occurred in the anode polarization curve, i.e., up until the inflection point. In a similar fashion, the oxidant efficiency was obtained from cathode polarization data at load current density values of 5.5 and 11 mA cm<sup>-2</sup>.

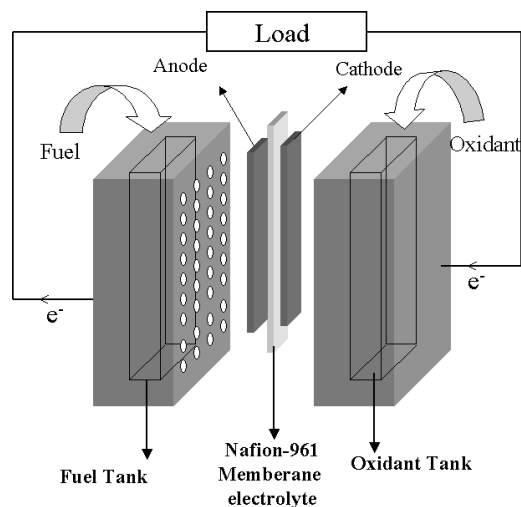


Fig. 1 Schematic diagram of a direct borohydride/hydrogen peroxide fuel cell.

## 3 Results and Discussion

A comparison of the cathode polarization data for DBFCs employing Nafion<sup>®</sup>-117 and Nafion<sup>®</sup>-961 with gold cathodes is shown in Figure 2. The data clearly show an improved cathodic polarization for the DBFC with the Nafion<sup>®</sup>-961 membrane electrolyte, suggesting a reduction in the alkali crossover across the Nafion<sup>®</sup>-961 membrane. Moreover, at the end of the experiment, the pH in the catholyte compartment of the DBFC was ~12, while employing Nafion<sup>®</sup>-117 as the electrolyte, a result of which was the rapid decline in the cathode potential on operation of the cell. The Nafion<sup>®</sup>-961 membrane reduces the crossover of aqueous NaOH from the anode to the cathode in the cell. Accordingly, the catholyte pH never exceeds 3, aiding an increase in oxidant utilization with an associated reduction in cathode polarization. This

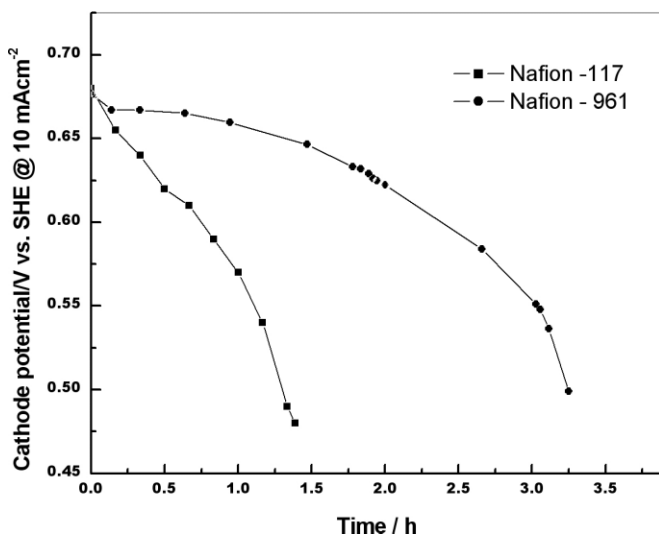


Fig. 2 Comparison of cathode polarization data for DBFCs employing Nafion®-117 and Nafion®-961 electrolyte membranes as electrolyte with gold cathodes.

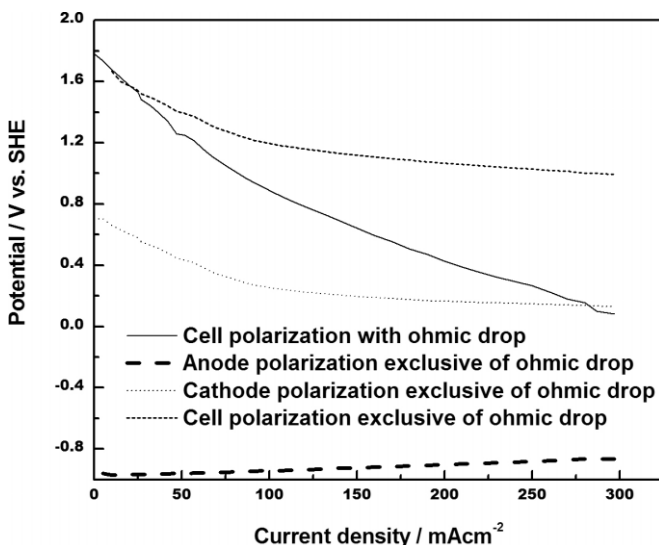


Fig. 3 Cell polarization data for the direct borohydride/hydrogen peroxide fuel cell with and without an ohmic component, and its anode and cathode polarization data without any ohmic drop across the membrane.

is because  $\text{PbSO}_4/\text{C}$  only catalyzes hydrogen peroxide reduction in acidic media, according to Reactions (15) and (17) [39]. This reflects an increase in  $\text{pH}$  due to proton consumption and an increase in concentration polarization as the hydrogen peroxide is consumed, as the reaction proceeds. However, note that lead sulfate does not dissolve in the acidified hydrogen peroxide solution, as the  $\text{pH}$  for hydrogen peroxide remains below 3 throughout cell operation. The ohmic region in the cell polarization curve, shown in Figure 3, lies beyond  $25 \text{ mA cm}^{-2}$ . The high resistance, about  $3 \text{ ohm cm}^2$ , observed for the cell is due to the low specific  $\text{Na}^+$ -ion conductivity for Nafion®-961 ( $2.33 \times 10^{-3} \text{ ohm}^{-1} \text{ cm}^{-1}$  at  $25 \text{ }^\circ\text{C}$ ) compared to that for Nafion®-117 ( $5.4 \times 10^{-3} \text{ ohm}^{-1} \text{ cm}^{-1}$  at  $25 \text{ }^\circ\text{C}$ ), in addition to the ohmic drop across the liquid junction, between the alkali and acid interface, within the mem-

brane and sluggish kinetics for  $\text{H}_2\text{O}_2$  reduction on  $\text{PbSO}_4/\text{C}$ . The cell polarization curve, corrected for the ohmic drop, is also included in Figure 3.

The performance data for the direct borohydride/hydrogen peroxide fuel cell, along with its anode and cathode data, are shown in Figure 3. The rapid polarization data in Figure 3 was obtained in steps of  $0.25 \text{ mA s}^{-1}$  up to  $100 \text{ mA}$  and subsequently in steps of  $0.5 \text{ mA s}^{-1}$  until the end of the experiment, in order to avoid any appreciable change in the catholyte  $\text{pH}$ . The individual electrode potentials exclude potential drops across the membrane, as these were measured by placing reference electrodes in the respective tanks. Figure 4 shows current polarization and power-density data for the cell. A peak power-density of about  $10 \text{ mW cm}^{-2}$  was achieved at  $0.77 \text{ V}$ , while operating the cell at  $25 \text{ }^\circ\text{C}$ . Coulombic efficiency values for borohydride oxidation on the misch-metal alloy anode were obtained from anode polarization data, at load current density values of  $11$  and  $23 \text{ mA cm}^{-2}$ , as shown in Figure 5a. Similarly, coulombic efficiency values for hydrogen peroxide reduction on the  $\text{PbSO}_4/\text{C}$  cathode were obtained from cathode polarization data at load current density values of  $5.5$  and  $11 \text{ mA cm}^{-2}$ , as shown in Figure 5b. The borohydride utilization efficiency<sup>1</sup> increases from  $19\%$  to  $23\%$ , while increasing the load current density from  $11$  to  $23 \text{ mA cm}^{-2}$ . For a DMFC operating at  $100 \text{ }^\circ\text{C}$ , a coulombic efficiency of about  $56\%$  has been reported in the literature [56]. Unlike the  $\text{NaBH}_4/\text{H}_2\text{O}_2$  fuel cell reported here, DMFCs employ noble metal catalysts for both methanol oxidation and oxygen reduction. DMFCs are also limited by methanol crossover and the generation of  $\text{CO}_2$ .

A major drawback of the DBFC is the associated evolution of hydrogen during the electrooxidation of borohydride, the relative rates of which depend on the anodic materials, applied potentials, and chemical states of the anodic surfaces. Borohydride undergoes hydrolysis in the presence of misch-metal alloy even at the open-circuit potential. Accordingly, the electrochemical utilization of borohydride depends on its rate of utilization. For this reason, borohydride utilization increases with increasing load current density. In contrast, hydrogen peroxide is found to be more stable on the  $\text{PbSO}_4/\text{C}$  cathode, with a utilization efficiency of  $74\%$  to  $80\%$  at load current densities between  $5.5$  and  $11 \text{ mA cm}^{-2}$ . While polarizing the cell at a load current density of  $11 \text{ mA cm}^{-2}$ , oxygen evolution on the  $\text{PbSO}_4/\text{C}$  surface, due to the chemical decomposition of  $\text{H}_2\text{O}_2$ , proceeds slowly, at  $3 \times 10^{-8} \text{ mol s}^{-1}$  as compared to a value of  $5.9 \times 10^{-6} \text{ mol s}^{-1}$  observed for platinum [40]. This justifies the suitability of  $\text{PbSO}_4/\text{C}$  for  $\text{H}_2\text{O}_2$  reduction in acidic media, compared to platinum, for the potential regime investigated in this study.

The long-term performance of the DBFC, studied by polarizing it at a load current density of  $5.5 \text{ mA cm}^{-2}$ , is shown in

<sup>1</sup> Utilization efficiency (in %) of sodium borohydride = (Amount of borohydride utilized for electrical work / Amount of borohydride injected)  $\times 100$

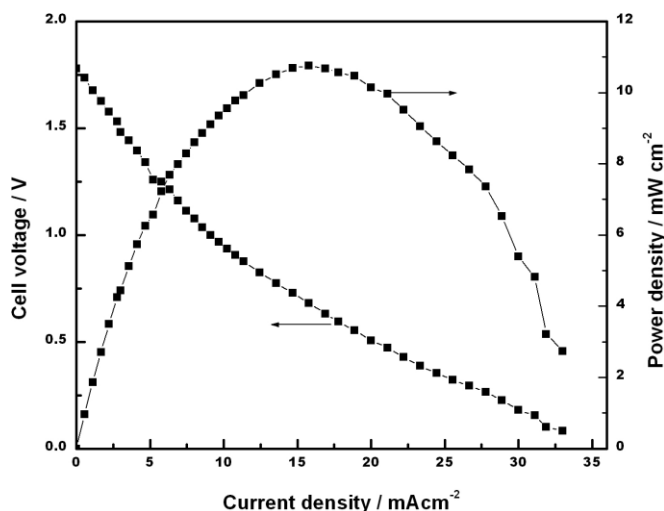


Fig. 4 Galvanostatic polarization data for a direct borohydride/hydrogen peroxide fuel cell along with the variation in its power density.

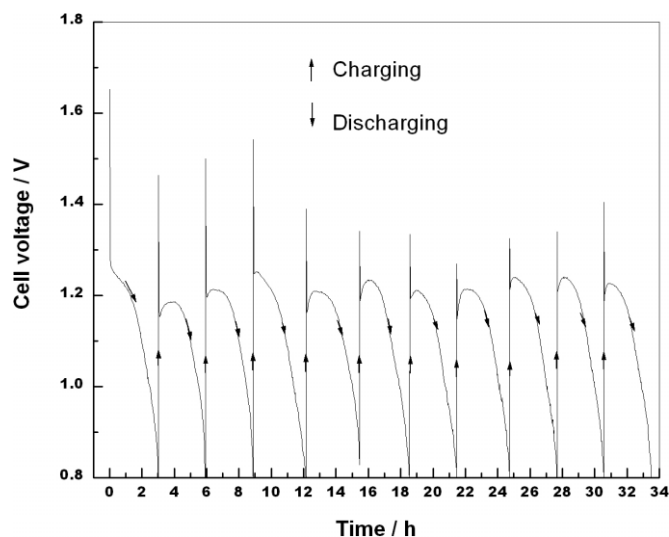


Fig. 6 Performance data for a direct borohydride/hydrogen peroxide fuel cell at a load current density of  $5.5 \text{ mA cm}^{-2}$ .

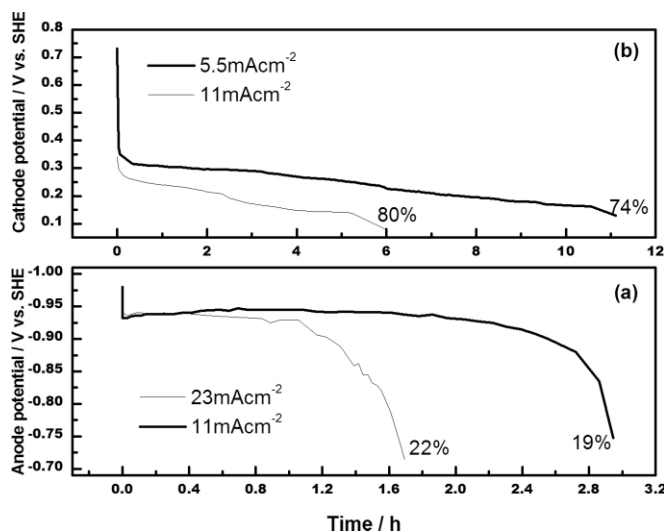


Fig. 5 Coulombic efficiency data for (a) sodium borohydride oxidation on a misch-metal alloy and (b) hydrogen peroxide reduction on a  $\text{PbSO}_4/\text{C}$  cathode in the direct borohydride/hydrogen peroxide fuel cell.

Figure 6. During the performance test, the DBFC was replenished with fuel and oxidant when its potential reached 0.8 V. In practice, portable fuel cells, e.g., batteries are limited by the amount of reactant, as these are contained within the device. Therefore, the cell has to be operated like a battery, where the replenishment of reactants in the cell is referred to as charging and their expending as discharging, as indicated in Figure 6. The charge and discharge data obtained over ten charge-discharge cycles show little deterioration in the performance of the DBFC. However, note that the stability of the  $\text{PbSO}_4$  under these conditions is of concern, as the reaction



occurs inherently at the cathode. It is possible to enhance a  $\text{PbSO}_4$ -based DBFC that could operate continuously for a pro-

longed period, as shown in Figure 6. The stability of the catalysts in the given environment was ascertained, since the DBFC operates for the same duration for each recharge.

It is also significant that the open-circuit voltage of  $\sim 1.8 \text{ V}$  for the direct borohydride/hydrogen peroxide fuel cell reported here is only 60% of the theoretical open-circuit voltage. Consequently, finding an anode that oxidizes the borohydride close to its thermodynamic equilibrium potential with less associated hydrogen evolution and a cathode that reduces hydrogen peroxide near its thermodynamic equilibrium potential with less associated oxygen evolution, would undoubtedly be beneficial for both hydrogen/air and methanol/air fuel cells that have open-circuit voltages of  $\sim 1 \text{ V}$  and  $\sim 0.8 \text{ V}$ . These voltages are about 80% and 65% of the respective thermodynamic equilibrium voltages. In addition, the specific energy of  $9.3 \text{ kWh kg}^{-1}$  for sodium borohydride compares favorably with the value of  $6.1 \text{ kWh kg}^{-1}$  for methanol. These data are encouraging for the exploitation of direct borohydride/hydrogen peroxide fuel cells in contemporary portable devices in places where anaerobic conditions prevail, e.g., in submersible and space applications.

## 4 Conclusions

The performance of a direct borohydride/hydrogen peroxide fuel cell operating as a battery at a load current density of  $5.5 \text{ mA cm}^{-2}$  was reported. The use of a Nafion<sup>®</sup>-961 electrolyte membrane in the cell reduced alkali crossover from the anode to cathode, increasing oxidant utilization. These properties make the borohydride/hydrogen peroxide fuel cell an attractive candidate for certain submersible and space applications.

## Acknowledgements

Financial assistance from the Council of Scientific and Industrial Research, New Delhi is gratefully acknowledged. Dr. R. A. Mashelkar, F.R.S. is thanked for his keen interest and encouragement.

## References

- [1] R. Farrauto, S. Hwang, L. Shore, W. Ruettinger, J. Lampert, T. Giroux, Y. Liu, O. Ilinich, *Annu. Rev. Mater. Res.* **2003**, *33*, 1.
- [2] H. P. Dhar, L. G. Christner, A. K. Kush, H. C. Maru, *J. Electrochem. Soc.* **1986**, *133*, 1574.
- [3] G. Hoogers, *Fuel cell technology handbook*, CRC Press, New York, **2003**.
- [4] A. K. Shukla, A. S. Aricò, V. Antonucci, *Renewable Sustainable Energy Rev.*, **2001**, *5*, 137.
- [5] C. Lamy, A. Lima, V. Le Rhun, C. Coutnneau, J. M. Leger *J. Power Sources* **2002**, *105*, 283.
- [6] A. Hamnett, *Catal. Today* **1997**, *38*, 445.
- [7] E. Reddington, A. Sapienza, B. Gurau, R. Viswanathan, S. Sarangapani, E. S. Smotkin, T. E. Mallouk, *Science* **1998**, *280*, 1735.
- [8] A. Heinzel, V. M. Barragán, *J. Power Sources* **1999**, *84*, 70.
- [9] J. Larminie, A. Dicks, *Fuel Cell Systems Explained*, Wiley, New York, **2003**.
- [10] www.qinetiq.com
- [11] S. S. Srinivasan, H. W. Brinks, B. C. Hauback, D. Sun, C. M. Jensen, *J. Alloys Compd.* **2004**, *377*, 283.
- [12] P. Wang, C. M. Jensen, *J. Alloys Compd.* **2004**, *379*, 99.
- [13] M. E. Indig, R. N. Snyder, *J. Electrochem. Soc.* **1962**, *109*, 1104.
- [14] M. Jung, H. H. Kroeger, *US Patent 3511710*, **1970**.
- [15] J.-Y. Lee, H. H. Lee, J. H. Lee, D. M. Kim, *US Patent 5599640*, **1997**.
- [16] S. C. Amendola, *US Patent 5804329*, **1998**.
- [17] S. C. Amendola, P. Onnerud, M. T. Kelly, P. J. Petillo, S. L. Sharp-Goldman, M. Binder, *J. Power Sources* **1999**, *84*, 130.
- [18] S. Suda, *US Patent 6358488*, **2002**.
- [19] Z. P. Li, B. H. Liu, K. Arai, S. Suda, *J. Electrochem. Soc.* **2003**, *150*, A868.
- [20] Z. P. Li, B. H. Liu, K. Arai, K. Asaba, S. Suda, *J. Power Sources* **2004**, *126*, 28.
- [21] B. H. Liu, Z. P. Li, S. Suda, *Electrochim. Acta* **2004**, *49*, 3097.
- [22] Z. P. Li, B. H. Liu, K. Arai, S. Suda, *J. Alloys and Compounds* **2005**, *404–406*, 648.
- [23] L. Wang, C.-A. Ma, X. Mao, J. Sheng, F. Bai, F. Tang, *Electrochem. Comm.* **2005**, *7*, 1477.
- [24] N. A. Choudhury, R. K. Raman, S. Sampath, A. K. Shukla, *J. Power Sources* **2005**, *143*, 1.
- [25] M. H. Atwan, C. L. B. Macdonald, D. O. Northwood, E. L. Gyenge, *J. Power Sources* **2006**, *158*, 36.
- [26] E. Gyenge, M. Atwan, D. Northwood, *J. Electrochem. Soc.* **2006**, *153*, A150.
- [27] J.-H. Wee, *J. Power Sources* **2006**, *155*, 329.
- [28] D. Hua, Y. Hanxi, A. Xinping, C. Chuansin, *Int. J. Hydrogen Energy* **2003**, *28*, 1095.
- [29] Z. T. Xia, S. H. Chan, *J. Power Sources* **2005**, *152*, 46.
- [30] R. Jasinski, *Electrochem. Technol.* **1965**, *3*, 40.
- [31] M. Kubokawa, M. Yamashita, K. Abe, *Denki Kagaku Oyobi Kogyo Butsuri Kagaku* **1968**, *36*, 778.
- [32] J. P. Elder, A. Hickling, *Trans. Faraday Soc.* **1962**, *58*, 1852.
- [33] H. Dong, R. X. Feng, X. P. Ai, Y. L. Cao, H. X. Yang, C. Cha, *J. Phys. Chem.* **2005**, *B 109*, 10896.
- [34] E. Gyenge, *Electrochim. Acta* **2004**, *49*, 965.
- [35] L. Wang, C. Ma, X. Mao, *J. Alloys and Compounds* **2005**, *397*, 313.
- [36] C. Ponce de Leon, F. C. Walsh, D. Pletcher, D. J. Brownling, J. B. Lakeman, *J. Power Sources* **2006**, *155*, 172.
- [37] H. Cheng, K. Scott, *Electrochim. Acta* **2006**, *51*, 3429.
- [38] R. X. Feng, H. Dong, Y. D. Wang, X. P. Ai, Y. L. Cao, H. X. Yang, *Electrochemistry Communications* **2005**, *7*, 449.
- [39] R. K. Raman, A. K. Shukla, *J. Applied Electrochemistry* **2005**, *35*, 1157.
- [40] R. K. Raman, N. A. Choudhury, A. K. Shukla, *Electrochem. and Solid-State Lett.* **2004**, *7*, A488.
- [41] K. Kordesch, G. Simader, *Fuel Cells and their Applications*, VCH, Weinheim, **1996**.
- [42] D. R. Lide, *Handbook of Chemistry and Physics*, CRC Press, Washington D.C., **1998-99**.
- [43] D. N. Prater, J. J. Rusek, *Appl. Energy* **2003**, *74*, 135.
- [44] H. I. Schlesinger, H. C. Brown, A. E. Finholt, *J. Am. Chem. Soc.* **1953**, *75*, 205.
- [45] R. C. Wade in *Specialty Inorganic Chemicals*, (Ed. R. Thomson), Royal Society of Chemistry, London, **1981**, pp. 25.
- [46] G. Broja, W. Schlabacher, *DE Patent 1108670*, **1959**.
- [47] F. Schubert, K. Lang, W. Schlabacher, *DE Patent 1067005*, **1959**.
- [48] S. Suda in *Handbook of Fuel Cells: Fundamentals Technology and Applications*, (Eds. W. Vielstich, A. Lamm, H. A. Gasteiger), Wiley, Chichester, **2003**, pp. 115.
- [49] T. Haga, Y. Kojima, *JP Patent 2002-241109*, **2002**.
- [50] Y. Kojima, T. Haga, K. Suzuki, H. Hayashi, S. Matsumoto, H. Nakanishi, *JP Patent 2002-193604*, **2002**.
- [51] Y. Kojima, T. Haga, *Int. J. Hydrogen Energy* **2003**, *28*, 989.
- [52] Z. P. Li, B. H. Liu, N. Morigasaki, S. Suda, *J. Alloys Compd.* **2003**, *354*, 243.
- [53] Z. P. Li, N. Morigasaki, B. H. Liu, S. Suda, *J. alloys Compd.* **2003**, *349*, 232.
- [54] S. Suda, *JP Patent 2002-173306*, **2002**.
- [55] J. C. Prager in *Environmental Contaminant Reference Data Book, Vol. 1-3*, John Wiley&Sons, New York, **1998**.
- [56] A. K. Shukla, P. A. Christensen, A. Hamnett, M. P. Ho-garth, *J. Power Sources* **1995**, *55*, 87.